Band structure and edge states of star-like zigzag graphene nanoribbons*

Hong Liu(刘红)†

Physics Department of Nanjing Normal University, Nanjing 210023, *China*

(Received 10 March 2017; revised manuscript received 6 August 2017; published online 30 September 2017)

Connecting three zigzag graphene nanoribbons (ZGNRs) together through the sp^3 hybrid bonds forms a star-like ZGNR (S-ZGNR). Its band structure shows that there are four edge states at $k = 0.5$, in which the three electrons distribute at three outside edge sites, and the last electron is shared equally (50%) by two sites near the central site. The lowest conductance step in the valley is 2, two times higher than that of monolayer ZGNR (M-ZGNR). Furthermore, in one quasi-three-dimensional hexagonal lattice built, both of the Dirac points and the zero-energy states appear in the band structure along the z-axis for the fixed zero k-point in the x–y plane. In addition, it is an insulator in the x–y plane due to band gap 4 eV, however, for any k-point in the x–y plane the zero-energy states always exist at $k_z = 0.5$.

Keywords: zigzag graphene nanoribbon, band structure, edge state

PACS: 73.22.Pr, 73.90.+f, 73.63.–b **DOI:** 10.1088/1674-1056/26/11/117301

1. Introduction

Since the discovery of carbon nanotubes (CNTs)[1] and the ground breaking experiments regarding monolayer graphene,[2] the low-dimensional carbon nano-material has become a promising material for future electronics. Extensive experimental and theoretical researches have been devoted to the study of their various novel physical properties. The subsequent experimental measurement on graphene layers excited the investgation on the spin quantum transport.[3,4] Recently, topological surface states (edge states) in condensed matter have received a lot of attention. Specially zigzag-edged graphene nanoribbons (ZGNRs) have recently received significant attention due to their unique spin-related electronic structures and topologically-protected edge states.[5–11] Sheng *et al.* proposed that the quantum spin Hall effect (QSHE)[12–15] can occur in the topoligical insulaters (TIs) without the applied magnetic field.[16–22]

Nowadays, many experimental and theoretical studies focus on looking for new types of two-dimensional layered materials to find new two-dimensional TIs that have a large bulk energy gap for QSHE in practice. Recently, many new two-dimensional TIs have been found, such as HgTe/CdTe,[17] InAs/GaSb,[18] and Cd_3As_2 quantum-well structures,[18] Bi_2TeI,[19] the bismuth (111) bilayer,[20] and the simple binary compounds $ZrTe_5$ and $HfTe_5$.[21,22] However, by using the known two-dimensional TIs, especially the two-dimensional graphene, the assembled quasi-one-dimensional materials are little studied. In 2015, Weng *et al.* proposed three-dimensional graphene networks with negative curvature, which have the topologically nontrivial node lines in bulk based on the first-principle calculations.[23]

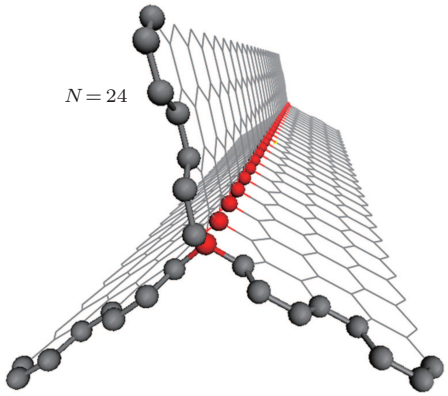


Fig. 1. (color online) The structure of star-like ZGNR. N is the number of carbon atoms in the primitive cell denoted as the gray balls. The red balls show those atoms having four nearest-neighbor sites bonded through the sp^3 hybrid orbits.

As is well known, the ZGNRs have topologically-protected edge states, we are interested in the properties of the assembled carbon nanomaterials (ACNMs) built up by several ZGNRs. This exciting idea can help us construct new artificial materials or devices with much more expected function effects. Obviously, these ACNMs have the stable geometrical structure and can be producted artificially due to the various bond configurations of carbon atoms connecting to their neighbor atoms. In the present work, we try to assemble three ZGNRs as one star-like new quasi-one-dimensional carbon nanomaterial shown in Fig. 1, called star-like ZGNR (S-ZGNR). We have optimized it by using the empirical potential. The S-ZGNR may not only have the merit characters inherited from graphene, but also have some novel effects due to the existence of the sp^3 hybrid bonds connecting the three ZGNRs. In this regard, we believe that this type of ACNM is one exciting nanomaterial system for the design of quasi-one-

*Project supported by the National Natural Science Foundation of China (Grant No. 10947004) and the Jiangsu Government Scholarship for Overseas Studies, China.

†Corresponding author. E-mail: liuhong3@njnu.edu.cn

© 2017 Chinese Physical Society and IOP Publishing Ltd

dimensional or quasi-three-dimensional nano-device working in the lower energy region.

2. Electric structure and quantum conductance

With the π-electron tight-binding method only considering the nearest neighbors, the band structure of S-ZGNR is shown in Fig. 2(a). The Hamiltonian of the system is written as

$$H = \sum_{\langle i,j \rangle} t_{ij}(c_i^+ c_j + \text{h.c.}), \tag{1}$$

where c_i^+ (c_i) is the electron creation (annihilation) operator at site i, and the hopping parameter is $t_{ij} = t_0 = -2.75$ eV. $\sum_{\langle i,j \rangle}$ denotes the summation over the nearest-neighbor sites. Because the model neglects the influence of the bond length and the angle between two bonds on the hopping parameter, the differences in band structure are caused by the bond configuration in S-ZGNR. The band structure of the corresponding monolayer ZGNR (M-ZGNR) with the same size ($N = 24$) is shown in Fig. 2(b) for comparison.

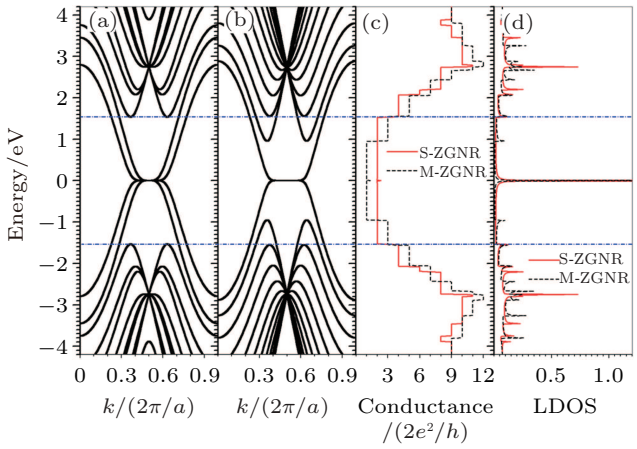


Fig. 2. (color online) The electronic structures and quantum conductance of S-ZGNR and M-ZGNR with the same size $N = 24$: the band structures of (a) S-ZGNR and (b) M-ZGNR, (c) the quantum conductance, (d) the local density of states (LDOS).

Naturally, in the energy region away from the Fermi energy, the band structure in Fig. 2(a) is similar to that of the M-ZGNR. The main differences are found in the energy region of interest, near the Fermi energy. The bulk band gap is 3.0 eV from -1.5 eV to 1.5 eV, larger than 2.0 eV in M-ZGNR. Furthermore, omitting the spin degree, one remarkable difference is that the number of bands drifting to the zero Fermi energy is 4, two times of that of M-ZGNR. In order to illustrate the edge-distribution charateristics of the states in these four bands drifiting to the zero Fermi energy, the spacial distribution of the electrons in these four states at $k = 0.5$ is shown in Fig. 3. At the outside sites 1, 11, and 17, denoted by the big red balls in Fig. 3, the occupied probability is 100% for the three electrons. Near the center site 14 of S-ZGNR, the two sites 13 and 24 share equally 50% of the fourth electron.

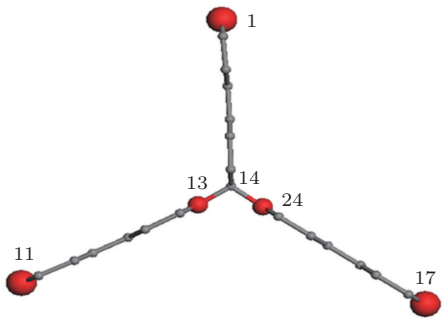


Fig. 3. (color online) The occupied probabilities of electrons in the four edge states at $k = 0.5$ in S-ZGNR. Three edge sites 1, 11, and 17 are denoted by big red balls with the probability 100%, and the two sites 13 and 24 are denoted by small red balls with the probability 50%.

By using the Landauer formula and Green's function method,[23–27] the quantum conductance through a region of interacting electrons can be calculated as

$$\mathscr{T} = 2\left(\frac{e^2}{h}\right)\text{tr}(\Gamma_\text{L} G_\text{C}^\text{r} \Gamma_\text{R} G_\text{C}^\text{a}), \tag{2}$$

where $\text{tr}(\Gamma_\text{L} G_\text{C}^\text{r} \Gamma_\text{R} G_\text{C}^\text{a})$ is the transmission function, $G_\text{C}^{\text{r,a}}$ represent the retarded and advanced Green functions of the heterojunction, and $\Gamma_{\text{L,R}}$ are the couplings of the heterojunction to the left and the right leads, respectively. In Fig. 2(c), comparing S-ZGNR with the M-ZGNR ($N = 24$), in the high energy region the quantum conductance steps are similar to the black dotted line for the M-ZGNR. Specially, in the low energy region of interest from -1.5 eV to 1.5 eV, the lowest quantum conductance step at the valley is 2, which is two times higher than that of M-ZGNR. Obviously, this higher step is attributed to there being more edge states. At the Fermi energy, the analysis of quantum conductance density at every site in the unit cell shows that at sites 11 and 17 the conductance is 0.4, and it is 0.32 at site 1. It is 0.25 little lower at the sites 13 and 24. The total of quantum conductance at these five sites is about 80% of the conductance step 2, which is in agreement with the characteristics of edge states in the band structure and the LDOS in Figs. 2(a) and 2(d).

Subsequently, using this S-ZGNR, we construct a quasi-three-dimensional lattice shown in Fig. 4(a). The corresponding reciprocal space structure is shown in Fig. 4(b). For some fixed special k points in the x–y plane shown in Fig. 4(b), the band structures varying with the k points along the z-axis are shown in Fig. 5.

In Fig. 5, an obvious common feature is the zero-energy states near $k_z = 0.5$. The subsequent calculations show that the zero-energy states always exist at $k_z = 0.5$ for any x–y plane k-point. However, there are many obvious differences in the band structures for the different fixed special wave vectors in the x–y plane. Among the figures in Fig. 5, one remarkable difference is the ocuurance of two Dirac points at $k_z = 0.315$ and 0.685 in Fig. 5(c) for the fixed zero point in the x–y plane. For $k_x = k_y = 0$, both of the two Dirac points and the zero-energy states exist near $k_z = 0.5$. In addition, apart from the special k points on the z-axis, the band structures in the x–y plane all

have a large band gap about 4.0 eV. Thus, the quantum conductance of this quasi-three-dimensional ACNM is anisotropy, it is an insulator in the x–y plane, but it is a conductor along the z-axis.

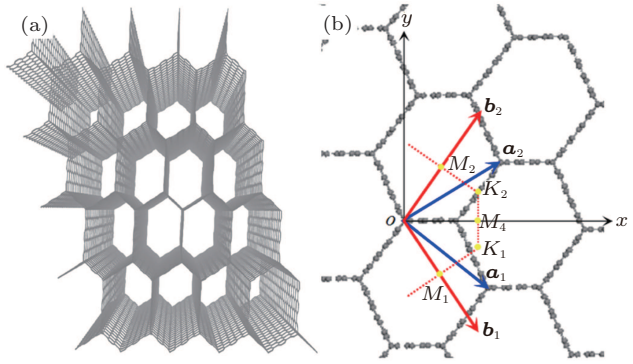


Fig. 4. (color online) (a) The geometrical structure and (b) the reciprocal space structure of quasi-three dimensional S-ZGNR. The high symmetrical k points are M_1, M_2, M_4, K_1, and K_2. The blue/red arrows show the unit vectors in real-space/reciprocal space in the x–y plane.

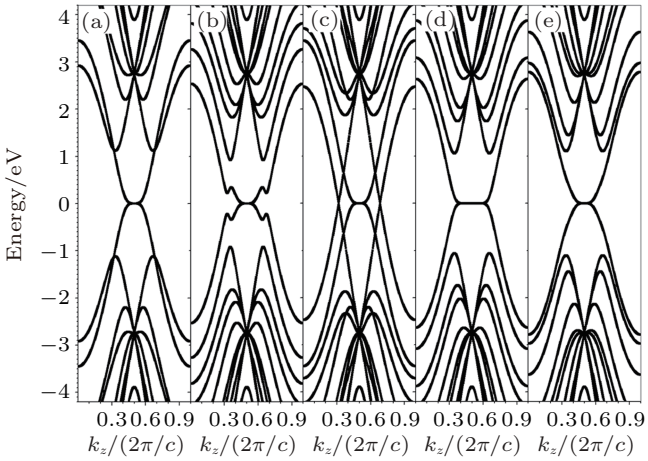


Fig. 5. The band structures along the z-axis k-point for five fixed x–y plane k points: (a) M_4, (b) $0.5M_1$, (c) $k_x = k_y = 0$, (d) M_1, (e) K_1.

3. Conclusions

For the assembled S-ZGNRs, there are four edge states at $k = 0.5$. The corresponding occupied probabilities are 100% at three outside edge sites, and 50% at two sites near the central site. We find that the lowest conductance step in the valley is 2, two times higher than that of M-ZGNR. At zero Fermi energy, the conductance density mainly concentrates at the same three outside edge sites. Furthermore, based on the geometrical structure of S-ZGNR, we build one quasi-three-dimensional hexagonal lattice. The Dirac points appear in the band structure for the fixed zero k-point in the x–y plane. For any k point in the x–y plane, there are zero-energy states at $k_z = 0.5$. Therefore, this quasi-three-dimensional all-carbon nanomaterial has high quantum conductance along the z-axis, but in the x–y plane it is an insulator due to the big band gap 4 eV in the band structure.

Obviously, for this assembled quasi-one-dimensional S-ZGNR and S-ZGNR hexagonal lattice, there are some novel zero-energy states. When introducing the on-site Coulomb interaction and the spin-orbital coupling, we expect that there are some interesting effects on the edge states and the Dirac points. Due to the large low-symmetrical primitive cell, it has super strong dipole matrix elements along the z-axis direction. Naturally, the strong nonlinear optical susceptibility and novel optical effect can be imaged for the incident light polarized along the z-axis direction. Furthermore, the lattice of quasi-three-dimensional hollow all-carbon nanomaterials is adjustable and can be artificially controlled. Therefore, in practical applications, we believe that this type of ACNM can be designed as a thermoelectronics, supercapacitor, hydrogen storage, absorbents, and strong nonlinear optical device.

Acknowledgment

The author is particularly grateful to her colleague Prof. Guiqin Huang for helping her to revise the Letter in English, and the initial discussion on the optimization of S-ZGNR from the first principle method.

References

[1] Iijima S 1991 *Nature* **354** 56
[2] Novoselov K S, Geim A K and Morozov S V 2005 *Nature* **438** 197
[3] Tombros N, Jozsa C, Popinciuc M, Jonkman H T and van Wees B J 2007 *Nature* **448** 571
[4] Williams J R, DiCarlo L and Marcus C M 2007 *Science* **317** 638
[5] Ezawa M 2006 *Phys. Rev. B* **73** 045432
[6] Fujita M, Wakabayashi K, Akada K and Kusakabe K 1996 *J. Phys. Soc. Jpn.* **65** 1920
[7] Nakada K, Fujita M, Dresselhaus G and Dresselhaus M S 1996 *Phys. Rev. B* **54** 17954
[8] Yang L, Cohen M L and Louie S G 2008 *Phys. Rev. Lett.* **101** 186401
[9] Wakayabashi K, Fujita M, Ajiki H and Sigrist M 1999 *Phys. Rev. B* **59** 8271
[10] Yao W, Yang S and Niu Q 2009 *Phys. Rev. Lett.* **102** 096801
[11] Liu H, Hu B and Liu N 2016 *Phys. Lett. A* **380** 3738
[12] Bernevig B A, Hughes T L and Zhang S C 2006 *Science* **314** 1757
[13] Yang Y, Xu Z, Sheng L, Wang B G, Xing D Y and Sheng D N 2011 *Phys. Rev. Lett.* **107** 066602
[14] Li H, Sheng L and Xing D Y 2012 *Phys. Rev. Lett.* **108** 196806
[15] Sheng Li 2014 *Progress in Physics* **34** 1 (in Chinese)
[16] König M, Wiedmann S, Brüne C, Roth A, Buhmann H, Molenkamp L W, Qi X L and Zhang S C 2007 *Science* **318** 766
[17] Knez I, Du R R and Sullivan G 2011 *Phys. Rev. Lett.* **107** 136603
[18] Sheng L 2013 *Progress in Physics* **34** 10
[19] Tang P, Yan B, Cao W, Wu S C, Felser C and Duan W 2014 *Phys. Rev. B* **89** 041409(R)
[20] Murakami S 2006 *Phys. Rev. Lett.* **97** 236805
[21] Weng H, Dai X and Fang Z 2014 *Phys. Rev. X* **4** 011002
[22] Wu R, Ma J Z, Nie S M, Zhao L X, Huang X, Yin J X, Fu B B, Richard P, Chen G F, Fang Z, Dai X, Weng H M, Qian T, Ding H and Pan S H 2016 *Phys. Rev. X* **6** 021017
[23] Weng H, Liang Y, Xu Q, Yu R, Fang Z, Dai X and Kawazoe Y 2015 *Phys. Rev. B* **92** 045108
[24] Kubo R 1957 *J. Phys. Soc. Jpn.* **12** 570
[25] Nardelli M B 1999 *Phys. Rev. B* **60** 7828
[26] Ferreira M S, Dargam T G, Muniz R B and Latge A 2000 *Phys. Rev. B* **62** 16040
[27] Ferreira M S, Dargam T G, Muniz R B and Latge A 2001 *Phys. Rev. B* **63** 245111
[28] Nardelli M B and Bernholc J 1999 *Phys. Rev. B* **60** 16338